

Minimal dark matter in type III seesaw

Eung Jin Chun

Korea Institute for Advanced Study, Hoegiro 87, Dongdaemun-gu, Seoul 130-722, Korea

Email: ejchun@kias.re.kr

ABSTRACT: We explore the possibility of a new dark matter candidate in the supersymmetric type III seesaw mechanism where a neutral scalar component of the $Y=0$ triplet can be the lightest supersymmetric particle. Its thermal abundance can be in the right range if non-standard cosmology such as kination domination is assumed. The enhanced cross-section of the dark matter annihilation to W^+W^- can leave detectable astrophysical and cosmological signals whose current observational data puts a lower bound on the dark matter mass. The model predicts the existence of a charged scalar almost degenerate with the dark matter scalar and its lifetime lies between 5.5 cm and 6.3 m. It provides a novel opportunity of the dark matter mass measurement by identifying slowly-moving and highly-ionizing tracks in the LHC experiments. If the ordinary lightest supersymmetric particle is the usual Bino, its decay leads to clean signatures of same-sign di-lepton and di-charged-scalar associated with observable displaced vertices which are essentially background-free and can be fully reconstructed.

KEYWORDS: Beyond Standard Model, Supersymmetry Phenomenology, Neutrino Physics.

Contents

1. Introduction	1
2. Triplet spectrum in supersymmetric type III seesaw	2
3. Relic density and indirect detection limits	3
4. LHC signatures	6
5. Conclusion	8

1. Introduction

Dark matter (DM) candidates can be found in some well-motivated extensions of Standard Model. The best-known example would be Minimal Supersymmetric Standard Model (MSSM) with R-parity in which the lightest supersymmetric particle (LSP) turns out to be a good DM particle whose thermal relic density is naturally in the right range [1].

Low-energy supersymmetry at the TeV scale has been motivated as a natural explanation of the electroweak symmetry breaking, and it may also be related to the origin of neutrino masses. This motivates us to introduce into MSSM a TeV-scale seesaw mechanism explaining the observed neutrino masses and mixing. In this regard, it is interesting to address a question whether there can be a new dark matter candidate coming from the neutrino sector.

The most popular way to realize the seesaw mechanism [2] is to introduce massive singlet (right-handed) neutrinos (type I seesaw). In this case, the lightest right-handed sneutrino can be stable and become an additional candidate of dark matter whose relic density is determined non-thermally [3] or thermally if the right-handed neutrinos carry extra $U(1)'$ interaction [4] or Yukawa interaction associated with the Higgs sector [5]. Another option is to assume the presence of an $SU(2)_L$ triplet with $U(1)_Y$ charge one ($Y = 1$), which couple to two lepton doublets and thus generate neutrino masses through its small vacuum expectation value (type II seesaw). This model predicts quite distinctive collider signatures through which the structure of the neutrino mass matrix can be explored [6]. However, its dark matter candidate, the neutral component of the triplet fermion, directly couples to the Z gauge boson and thus its large coupling is already ruled out by direct detection experiments. The last option of our interest is to introduce $Y = 0$ triplets which couple to lepton and Higgs doublets (type III seesaw) [7]. A neutral scalar component of such triplet superfields can be the LSP. Let us remark that such a scalar triplet LSP can be another realization of the minimal dark matter studied in Ref. [8].

In the following, we explore properties of this scalar triplet present in the supersymmetric type III seesaw mechanism as a dark matter candidate and its signatures in collider experiments.

2. Triplet spectrum in supersymmetric type III seesaw

Type III seesaw mechanism introduces real $SU(2)_L$ triplets $\Sigma = (\Sigma^+, \Sigma^0, \Sigma^-)$ with $Y = 0$, which allows the superpotential,

$$W_{III} = y_{ij} L_i H_2 \Sigma_j + \frac{1}{2} M_k \Sigma_k \Sigma_k. \quad (2.1)$$

Integrating out the heavy triplet fields one obtains the seesaw neutrino mass matrix,

$$\mathcal{M}_{ij}^\nu = y_{ik} y_{jk} \frac{v_2^2}{M_k}, \quad (2.2)$$

where $v_2 = \langle H_2^0 \rangle$. From now on, the generation index for the triplets will be suppressed as we are interested in the one containing the lightest neutral scalar component. The fermion triplet components, denoted by $\Sigma^{\pm,0}$, have the common mass M . For the mass spectrum of the scalar triplet components, denoted by $\tilde{\Sigma}^{\pm,0}$, we need to consider the supersymmetric mass M , the soft supersymmetry breaking masses and the electroweak mass splitting. The neutral scalar components with $T_3 = 0$ take the masses given by

$$m_{\tilde{\Sigma}_{2,1}^0}^2 = M^2 + \tilde{m}^2 \pm BM \quad (2.3)$$

where \tilde{m} is the diagonal soft mass and B is the bilinear soft term which will be assumed to be positive without loss of generality. The charged scalar components $\tilde{\Sigma}^\pm$ carrying $T_3 = \pm 1$ have the following mass-squared matrix:

$$\mathcal{M}_{\tilde{\Sigma}^\pm}^2 = \begin{bmatrix} M^2 + \tilde{m}^2 + c_W^2 m_Z^2 c_{2\beta} & BM \\ BM & M^2 + \tilde{m}^2 - c_W^2 m_Z^2 c_{2\beta} \end{bmatrix}, \quad (2.4)$$

where c_W is the cosine of the weak mixing angle and the angle β is defined by $t_\beta = v_2/v_1$. Diagonalizing Eq. (2.4), one finds the mass-squared eigenvalues,

$$m_{\tilde{\Sigma}_{2,1}^\pm}^2 = M^2 + \tilde{m}^2 \pm \sqrt{B^2 M^2 + c_W^4 m_Z^4 c_{2\beta}^2}. \quad (2.5)$$

Note that the lighter scalars, $\tilde{\Sigma}_1^\pm$ and $\tilde{\Sigma}_1^0$, can have smaller masses than their fermionic partners and the ordinary superparticles ($m_{\tilde{\Sigma}_1} < M, \tilde{m}$) due to a large negative term driven by the B -term, and can be even lighter than the ordinary lightest supersymmetric particle (OLSP) in the MSSM. The tree-level mass splitting between $\tilde{\Sigma}_1^\pm$ and $\tilde{\Sigma}_1^0$ driven by the electroweak symmetry breaking is given by

$$\Delta m_{\text{tree}} \equiv [m_{\tilde{\Sigma}_1^\pm} - m_{\tilde{\Sigma}_1^0}]_{\text{tree}} \approx -\frac{c_W^2 m_Z^4 c_{2\beta}^2}{4BM m_{\tilde{\Sigma}_1^0}} \quad (2.6)$$

in the limit of $m_Z^2 \ll BM$. Note that the tree-level mass splitting is negative. On the other hand, one-loop correction induces positive contribution given by

$$\Delta m_{\text{loop}} = \frac{\alpha_2 m_{\tilde{\Sigma}_1^0}}{4\pi} [f(r_W) - c_W^2 f(r_Z)] \quad (2.7)$$

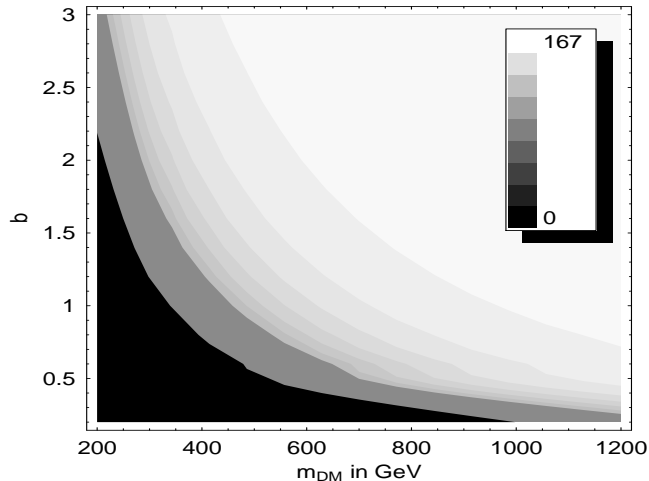


Figure 1: Contour plot of mass splitting Δm between the charged and the neutral (DM) scalar components as a function of the DM mass m_{DM} and the parameter $b \equiv \sqrt{BM}/m_{\text{DM}}$. The black region is for $\Delta m < 0$ and thus excluded for our discussion. In the next darkest region, we have $\Delta m < 100$ MeV, and Δm is increased by 10 MeV for each contour region. In the brightest region, Δm is larger than 160 MeV but below the upper limit of 167 MeV.

where $r_{W,Z} = m_{W,Z}/m_{\tilde{\Sigma}_1^0}$ and $f(r) = -r[2r^3 \ln r + (r^2 - 4)^{3/2} \ln(r^2 - 2 - r\sqrt{r^2 - 4})/2]/4$ [8].

The one-loop splitting reaches the typical maximum value $\Delta m_{\text{loop}} \approx 167$ MeV for $m_{\tilde{\Sigma}_1} \gg m_{W,Z}$ which can be partly cancelled by the tree-level splitting contribution. In Fig. 1, we show the total mass splitting $\Delta m = \Delta m^{\text{loop}} + \Delta m^{\text{tree}}$ in the plane of the lightest neutral scalar mass $m_{\text{DM}} = m_{\tilde{\Sigma}_1^0}$ and the dimensionless parameter $b \equiv \sqrt{BM}/m_{\text{DM}}$ quantifying the size of the B -term. Apart from the black region in the lower left corner, the neutral scalar component remains lighter than the charged scalar and can be the LSP dark matter. Depending on the size of Δm , some interesting collider signatures will occur as will be discussed in Section 4. Here let us remark that the

3. Relic density and indirect detection limits

The dominant annihilation channel of the dark matter, $\tilde{\Sigma}_1^0$, is the ‘direct’ gauge coupling with W^\pm , and thus it has a large s-wave annihilation rate [8]:

$$\langle \sigma v \rangle \approx \frac{4\pi\alpha_2^2}{m_{\tilde{\Sigma}_1^0}^2}. \quad (3.1)$$

It can give rise to the right thermal relic density only in the multi-TeV range in the standard cosmology. For smaller mass, the annihilation cross-section becomes large to suppress the standard thermal relic density. In this case, dark matter relics must come from a certain non-thermal origin, or from a non-standard thermal history of the universe. An interesting possibility for the latter is a kinetic energy (kination) domination driven

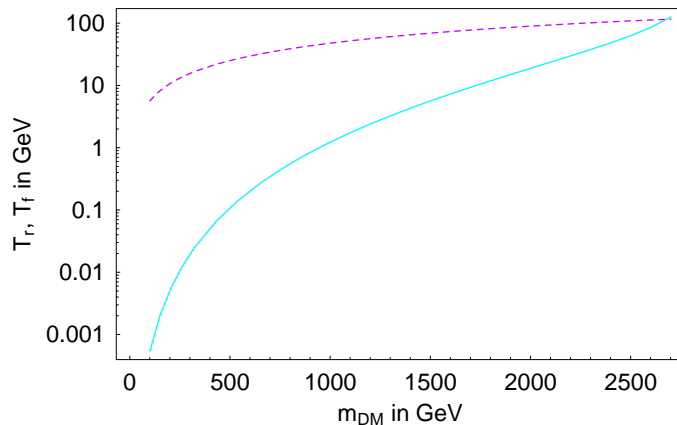


Figure 2: The solid line shows the reduced kination-radiation equality temperature, $T_r \equiv \sqrt{g_{*eq}/g_{*f}} T_{eq}$, required to produce the right dark matter density. The dotted line is the freeze-out temperature T_f .

by the evolution of quintessence which forms dark energy today [9]. Such a kination era would immediately follow the period of inflation in a cosmological scenario identifying the inflaton and quintessence field [10], where one can still find sufficient reheating through gravitational particle production [11].

For a phenomenological consideration of kination cosmology, it is enough to identify one free parameter T_{eq} at which the kination and radiation components become equal. At a given temperature T , the expansion parameter can be expressed as

$$H(T) = H_{st} \sqrt{1 + \frac{g_*}{g_{*eq}} \frac{T^2}{T_{eq}^2}} \quad (3.2)$$

where H_{st} is the Hubble parameter in the standard cosmology, $H_{st} \approx 1.66\sqrt{g_*}T^2/m_{pl}$. If dark matter freeze-out occurs before T_{eq} (when $H > H_{st}$), a larger annihilation cross-section is required to produce a right thermal relic density. Given the dark matter freeze-out temperature T_f and the kination-radiation equality temperature T_{eq} , one can find the approximate formula for the present dark matter density:

$$\Omega_{DM}h^2 \approx \frac{0.88 \times 10^{-10} \text{GeV}^{-2}}{\langle\sigma v\rangle} \frac{z_f}{\sqrt{g_{*f}}} k\left(\frac{z_r}{z_f}\right), \quad (3.3)$$

where $z_f = m_{\tilde{\Sigma}_1^0}/T_f$, $z_r = \sqrt{g_{*f}/g_{*eq}} m_{\tilde{\Sigma}_1^0}/T_{eq}$, and $k(u) = u/\ln(u + \sqrt{1+u^2})$ [14]. Note that the function k characterizing the kination domination recovers the standard value $k = 1$ in the limit of $u \rightarrow 0$. For the purpose of our investigation, we calculate T_f approximately by equating the annihilation cross-section and the expansion parameter. Then, requiring $\Omega_{DM}h^2 = 0.11$, one can find appropriate values of the freeze-out temperature T_f and the redefined kination-radiation equality temperature $T_r = \sqrt{g_{*eq}/g_{*f}} T_{eq}$ as functions of the dark matter mass $m_{\tilde{\Sigma}_1^0}$. The result is shown in Fig. 2. One finds that the required T_r is larger than about 5 MeV for the dark matter mass larger than 200 GeV, and thus there is no conflict with the standard big-bang nucleosynthesis in the parameter region of our interest.

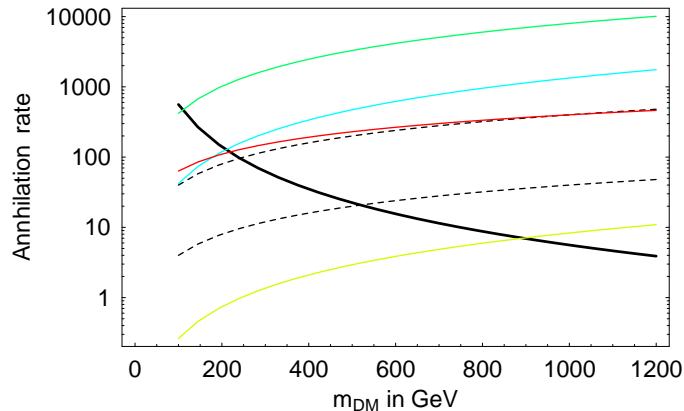


Figure 3: Thick solid line is the dark matter annihilation rate in unit of $3 \times 10^{-26} \text{ cm}^3/\text{sec}$. Solid lines from the upper most one show the constraints on the enhanced annihilation rate coming from the observations of extra-galactic diffuse gamma background [Belikov-Hooper [15]], big-bang nucleosynthesis [16], anti-proton flux in cosmic rays [17], and galactic center radio observation (assuming NFW profile) [18]. The upper (lower) dotted line is the limit from CMB measurement by WMAP5 (PLANCK) [19].

Concerning the direct detection of our dark matter particle, let us recall that it has $Q = Y = 0$ and its leading contribution to the scattering on nuclei comes from scalar interaction at one-loop. Thus its nucleonic cross-section is quite small: $\sigma_{\text{nucleon}} \approx 10^{-45} \text{ cm}^2$ [8], which is about two orders of magnitude below the current direct detection limit. It is amusing to note that our scalar dark matter triplet with $\Delta m \sim 10 \text{ MeV}$ can explain the DAMA/LIBRA modulation results [12] through the element-dependent resonant scattering [13].

The dark matter annihilation rate (3.1) of $\tilde{\Sigma}_1^0 \tilde{\Sigma}_1^0 \rightarrow W^+ W^-$ is much larger than the standard freeze-out value: $3 \times 10^{-26} \text{ cm}^3/\text{sec}$ for sub-TeV dark matter mass, as shown by the thick solid line in Fig. 3. Such an enhanced annihilation can lead to various indirect signals in astrophysics and cosmology, and thus gets restricted by current observational data. Fig. 3 summarizes various constraints analyzed in the recent literature considering the effects of dark matter annihilation to the extra-galactic diffuse gamma-ray background by produced energetic electrons and positrons [15], the changes in light element abundances predicted successfully by the big-bang nucleosynthesis [16], the anti-proton flux in cosmic rays [17], the radio observation from the galactic center [18], and the extra energy injection during the recombination epoch [19]. The most stringent limit comes from the galactic center radio observation which strongly depends on astrophysics models. The NFW profile is assumed for the lowest solid line which puts a strong bound: $m_{\tilde{\Sigma}_1^0} > 900 \text{ GeV}$. But, this bound disappears if the isothermal profile is assumed. Therefore, we do not take this bound for our consideration of collider signatures. The limits from the current CMB and anti-proton flux measurements are comparable. The WMAP5 bound reads

$$m_{\tilde{\Sigma}_1^0} > 240 \text{ GeV} \quad (3.4)$$

and the expected bound in PLANCK is $m_{\tilde{\Sigma}_1^0} > 520 \text{ GeV}$. Independently of such indirect

detection constraints, collider experiments will be able to provide another limit on the scalar triplet mass.

4. LHC signatures

Some of interesting collider signatures of neutrino mass models at TeV scale can occur in lepton-flavor violating decays of new particles responsible for generating light neutrino masses. They usually involve displaced vertices related to small neutrino masses and same-sign dilepton final states. In type III seesaw, the production of triplet fermions through off-shell W boson can yield such a signal: $pp \rightarrow \Sigma^\pm \Sigma^0 \rightarrow l^\pm l^\pm W^\mp Z^0$ [20, 21, 22, 23]. The decay rate of the triplet fermion is given by $\Gamma_\Sigma \approx y^2 M/8\pi$ where the neutrino Yukawa coupling can be traded with the effective neutrino mass: $\tilde{m}_\nu \equiv y^2 v_2^2/M$. Thus its lifetime becomes $\tau_\Sigma \approx 0.1$ mm for $\tilde{m}_\nu = 0.05$ eV and $M = v_2 \approx 174$ GeV. This result is applicable also to type I seesaw. In type II seesaw, where doubly charged Higgs boson decays to two same-sign leptons, the maximum decay length can be found to be about 0.3 mm [6].

In our DM scenario in supersymmetric type III seesaw, we concentrate on the collider phenomenology of the triplet scalars. A peculiar feature of displaced vertices reflecting small neutrino Yukawa couplings occurs now in the decay of the ordinary lightest supersymmetric particle. For our discussion, we will take the usual lightest neutralino χ_1^0 (mostly Bino) as the OLSP. Note that the seesaw mechanism in the fermion (scalar) sector induces mixing between lepton (slepton) doublets and fermion (scalar) triplets. In particular, two-body decays of the OLSP can arise through the mixing between sleptons and scalar triplets induced by the soft A -term and supersymmetric F -term,

$$V_{\text{mix}} = m_D A \left[\frac{1}{\sqrt{2}} \tilde{\nu} \tilde{\Sigma}^0 + \tilde{l} \tilde{\Sigma}^+ \right] + m_D M \left[\frac{1}{\sqrt{2}} \tilde{\nu} \tilde{\Sigma}^{0*} + \tilde{l} \tilde{\Sigma}^{-*} \right] + h.c., \quad (4.1)$$

where m_D denotes the Dirac neutrino mass between ν and Σ^0 : $m_D = yv_2$. The OLSP decay rates, for $\chi_1^0 \rightarrow l^\pm \tilde{\Sigma}_1^\mp$ and $\nu \tilde{\Sigma}_1^0$, are found to be

$$\begin{aligned} \Gamma(\chi_1^0 \rightarrow \nu \tilde{\Sigma}_1^0) &= \frac{\alpha'}{16} \theta_{\tilde{\nu}}^2 m_{\chi_1^0} \left(1 - \frac{m_{\tilde{\Sigma}_1}^2}{m_{\chi_1^0}^2} \right)^2, \\ \Gamma(\chi_1^0 \rightarrow l^\pm \tilde{\Sigma}_1^\mp) &= \frac{\alpha'}{32} \theta_l^2 m_{\chi_1^0} \left(1 - \frac{m_{\tilde{\Sigma}_1}^2}{m_{\chi_1^0}^2} \right)^2. \end{aligned} \quad (4.2)$$

Here the small parameters $\theta_{\tilde{l}, \tilde{\nu}}$ quantify the mixing between \tilde{l}^\pm ($\tilde{\nu}$) and $\tilde{\Sigma}_1^\pm$ ($\tilde{\Sigma}_1^0$):

$$\theta_{\tilde{l}, \tilde{\nu}} \approx \frac{M(M-A)}{m_{\tilde{l}, \tilde{\nu}}^2 - m_{\tilde{\Sigma}_1}^2} \delta \quad \text{where} \quad \delta \equiv \sqrt{\frac{\tilde{m}_\nu}{M}}. \quad (4.3)$$

Recall that δ is the small mixing angle between ν (l) and Σ^0 (Σ^-) coming from the seesaw relation $\tilde{m}_\nu = m_D^2/M$. Compared to the fermion triplet decay rate Γ_Σ discussed above, the OLSP decay rate (4.2), $\Gamma_{\chi_1^0} \approx \alpha' \delta^2 m_{\chi_1^0}/8$, is typically smaller by an order of magnitude,

and thus we expect to have more distinct displaced vertices. Taking again $\theta_{\tilde{l},\tilde{\nu}} \approx \delta$ and $\tilde{m}_\nu = 0.05$ eV, the OLSP decay length becomes

$$\tau_{\chi_1^0} \approx \left[\frac{\alpha'}{8} \tilde{m}_\nu \frac{m_{\chi_1^0}}{M} \right]^{-1} \approx 0.3 \text{ cm} \quad (4.4)$$

for $m_{\chi_1^0} = M$.

The charged and neutral scalar fields present in our model are nearly degenerate with each other. As shown in Section 1, the tree-level mass splitting driven by the B -term and D -term masses always gives negative contribution to $\Delta m = m_{\tilde{\Sigma}_1^\pm} - m_{\tilde{\Sigma}_1^0}$, which can partly cancel the positive one-loop correction. As a consequence of this, the mass splitting Δm can be smaller than the maximal splitting of $\Delta m \approx 167$ MeV induced solely by one-loop correction [8]. Depending on whether Δm is larger or smaller than m_{π^\pm} , one finds the allowed decay channel, $\tilde{\Sigma}_1^\pm \rightarrow \tilde{\Sigma}_1^0 \pi^\pm$ or $\tilde{\Sigma}_1^0 e^\pm \nu$, whose rates are given by [8]:

$$\begin{aligned} \Gamma(\tilde{\Sigma}_1^\pm \rightarrow \tilde{\Sigma}_1^0 \pi^\pm) &= \frac{2}{\pi} G_F^2 V_{ud}^2 \Delta m^3 f_\pi^2 \sqrt{1 - \frac{m_\pi^2}{\Delta m^2}}; \\ \Gamma(\tilde{\Sigma}_1^\pm \rightarrow \tilde{\Sigma}_1^0 e^\pm \nu) &= \frac{2}{15\pi^3} G_F^2 \Delta m^5. \end{aligned} \quad (4.5)$$

Note that we have a similar situation as in the Wino LSP scenario [24] with much more restricted value of Δm . Independently of the scalar triplet mass, the two-body decay rate takes its maximum value for $\Delta m \approx 167$ MeV, and its minimum value for $\Delta m = m_{\pi^\pm}$, below which the three body decay channel opens up. Unless the mass splitting Δm is finely tuned to be less than $m_{e^\pm} = 0.5$ MeV, the three body decay rate of Eq. (4.5) is applied for $\Delta m \leq m_{\pi^\pm}$. Thus, we restrict ourselves to the decay length of the charged scalar triplet in the range:

$$5.5 \text{ cm} \lesssim \Gamma_{\tilde{\Sigma}_1^\pm}^{-1} \lesssim 6.3 \text{ m}. \quad (4.6)$$

Recall that π^\pm or e^\pm from the $\tilde{\Sigma}_1^\pm$ decay is too soft to be observed in the LHC detectors. Thus one can only observe highly-ionizing tracks caused by $\tilde{\Sigma}_1^\pm$ which typically disappear somewhere inside a detector. When such a heavy charged particle moves slowly ($\beta < 1$), its momentum and velocity (and thus mass) can be measured simultaneously, providing a unique background-free and model-independent search for new physics. Experimental studies on the mass reconstruction have been performed by using the time-of-flight measurement at the muon detectors of ATLAS and CMS, and also by the ionization-rate (dE/dx) measurement at the tracker of CMS [26]. Both methods can be applied to our case if the mass splitting is close to or below m_{π^\pm} [see (4.6)].

The heavy scalar triplet $\tilde{\Sigma}_1^\pm$ can be produced following the (cascade) production of the OLSP:

$$pp \rightarrow \chi_1^0 \chi_1^0 \rightarrow \begin{cases} l^\pm l^\pm \tilde{\Sigma}_1^\mp \tilde{\Sigma}_1^\mp \\ l^\pm l^\mp \tilde{\Sigma}_1^\pm \tilde{\Sigma}_1^\mp \end{cases}, \quad (4.7)$$

or directly through W/Z boson exchange:

$$pp \rightarrow \begin{cases} \tilde{\Sigma}_1^\pm \tilde{\Sigma}_1^0 \\ \tilde{\Sigma}_1^+ \tilde{\Sigma}_1^- \end{cases}. \quad (4.8)$$

In the first case, one can have both the same-sign dileptons and same-sign anomalous charged tracks resulting from the Majorana nature of the mother particle. Note that the OLSP mass can be reconstructed from the energy (momentum) measurement of the charged leptons and the mass measurement of $\tilde{\Sigma}_1^\pm$. Furthermore, the reconstructed displaced vertices of the OLSP decay (4.4) can be useful to distinguish the candidate events. The production cross-section of the process (4.7) depends on models of supersymmetry breaking and sparticle mass spectrum. In addition to this, the process (4.8) can be used to test our model. Its production cross-section has been calculated in Ref. [25]. For $m_{\tilde{\Sigma}_1} = 250$ (800) GeV, the corresponding cross-sections for the $\tilde{\Sigma}_1^\pm \tilde{\Sigma}_1^0$ and $\tilde{\Sigma}_1^+ \tilde{\Sigma}_1^-$ productions are 60 (0.33) fb and 30 (0.16) fb, respectively. Therefore, anomalous charged tracks predicted by the type III seesaw dark matter model could be found at the early stage of the LHC luminosity of 10/fb if the scalar triplet is not too heavy; $m_{\tilde{\Sigma}_1} < 800$ GeV.

5. Conclusion

It is suggested that the neutral scalar component $\tilde{\Sigma}_1^0$ of the $Y=0$ triplet in the supersymmetric type III seesaw mechanism can be a viable dark matter candidate. The B -term contribution can lead to a large mass splitting between two neutral scalars and the lighter one becomes the LSP. For its mass in the sub-TeV range, the annihilation cross-section is much larger than the standard value 3×10^{-26} cm³/sec required for a thermal production of the observed relic density. Such an enhanced annihilation can be consistently accommodated by considering a non-standard cosmology: kination domination around the dark matter freeze-out era. This kind of scenario could be tested or limited indirectly through various astrophysical observations as summarized in Fig. 3. Currently the strongest bound comes from the radio observation from the galactic center which is however strongly dependent on the dark matter profile. Next stringent constraint is put by the WMAP5 CMB measurement, requiring $m_{\tilde{\Sigma}_1^0} > 240$ GeV.

A peculiar aspect of our model in view of collider phenomenology is the existence of the charged scalar particle $\tilde{\Sigma}_1^\pm$ which is almost degenerate with the dark matter particle $\tilde{\Sigma}_1^0$. Their mass splitting Δm gets both the (negative) tree-level and (positive) one-loop contributions which can cancel each other. When $\Delta m < m_{\pi^\pm}$, the charged scalar allows only three-body decay, $\tilde{\Sigma}_1^\pm \rightarrow \tilde{\Sigma}_1^0 e^\pm \nu$, with $\tau \approx 6.3$ m. This charged partner of the dark matter is another example of heavy long-lived charged particles whose mass can be measured model-independently by detecting their anomalous tracks in the LHC experiments. The charged scalars can be produced directly through the W/Z boson exchange, or after the production and the decay of the ordinary lightest supersymmetric particle like the Bino. In the latter case, we can probe clean signatures of same-sign di-lepton and di-charged-scalar tracks having measurable displaced vertices ($\tau \sim 0.3$ cm). Furthermore, the mass measurement of the charged scalars allows us to determine the OLSP mass as well. Let us remark that the direct production cross-section of our scalar particles is about 0.5 fb for the mass of 800 GeV. Thus discovery/exclusion of the model can be made up to $m_{\tilde{\Sigma}_1^0} < 800$ GeV with the integrated luminosity 10 fb⁻¹ as no background events are expected. Of course, one could observe much more events if a squark or gluino and thus the OLSP can

be copiously produced, which depends on the mass spectrum of heavier supersymmetric particles.

Acknowledgement: The author thanks Suyong Choi and Manuel Drees for valuable comments on the LHC signals. This work was supported by Korea Neutrino Research Center through National Research Foundation of Korea Grant (2009-0083526).

References

- [1] For a review, see, G. Jungman, M. Kamionkowski and K. Griest, *Phys. Rept.* **267**, 195 (1996) [arXiv:hep-ph/9506380].
- [2] For a review, see, R. N. Mohapatra *et al.*, “Theory of neutrinos: A white paper,” *Rept. Prog. Phys.* **70**, 1757 (2007) [arXiv:hep-ph/0510213].
- [3] T. Asaka, K. Ishiwata and T. Moroi, *Phys. Rev. D* **73**, 051301 (2006) [arXiv:hep-ph/0512118].
- [4] H.-S. Lee, K. T. Matchev and S. Nasri, *Phys. Rev. D* **76**, 041302 (2007) [arXiv:hep-ph/0702223].
- [5] D. G. Cerdeno, C. Munoz and O. Seto, *Phys. Rev. D* **79**, 023510 (2009) [arXiv:0807.3029 [hep-ph]]; F. Deppisch and A. Pilaftsis, *JHEP* **0810**, 080 (2008) [arXiv:0808.0490 [hep-ph]].
- [6] E. J. Chun, K. Y. Lee and S. C. Park, *Phys. Lett. B* **566**, 142 (2003) [arXiv:hep-ph/0304069].
- [7] R. Foot, H. Lew, X.-G. He and G. C. Joshi, *Z. Phys.* C44 (1989) 441.
- [8] M. Cirelli, N. Fornengo and A. Strumia, *Nucl. Phys. B* **753**, 178 (2006) [arXiv:hep-ph/0512090].
- [9] R. R. Caldwell, R. Dave and P. J. Steinhardt, *Phys. Rev. Lett.* **80** 1582 (1998) [arXiv:astro-ph/9708069]; P. J. Steinhardt, L. M. Wang and I. Zlatev, *Phys. Rev. D* **59** 123504 (1999) [arXiv:astro-ph/9812313].
- [10] B. Spokoiny, *Phys. Lett. B* **315** 40 [arXiv:gr-qc/9306008]; P. J. E. Peebles and A. Vilenkin, *Phys. Rev. D* **59** 063505 (1999) [arXiv:astro-ph/9810509].
- [11] L. H. Ford, *Phys. Rev. D* **35**, 2955 (1987); E. J. Chun, S. Scopel and I. Zaballa, *JCAP* **0907**, 022 (2009) [arXiv:0904.0675 [hep-ph]].
- [12] Y. Bai and P. J. Fox, arXiv:0909.2900 [hep-ph].
- [13] M. Pospelov and A. Ritz, *Phys. Rev. D* **78**, 055003 (2008) [arXiv:0803.2251 [hep-ph]].
- [14] P. Salati, *Phys. Lett. B* **571**, 121 (2003) [arXiv:astro-ph/0207396].
- [15] M. Kawasaki, K. Kohri and K. Nakayama, *Phys. Rev. D* **80**, 023517 (2009) [arXiv:0904.3626 [astro-ph.CO]]; S. Profumo and T. E. Jeltema, *JCAP* **0907**, 020 (2009) [arXiv:0906.0001 [astro-ph.CO]]; A. V. Belikov and D. Hooper, arXiv:0906.2251 [astro-ph.CO].
- [16] J. Hisano, M. Kawasaki, K. Kohri, T. Moroi and K. Nakayama, *Phys. Rev. D* **79**, 083522 (2009) [arXiv:0901.3582 [hep-ph]].
- [17] F. Donato, D. Maurin, P. Brun, T. Delahaye and P. Salati, *Phys. Rev. Lett.* **102**, 071301 (2009) [arXiv:0810.5292 [astro-ph]].
- [18] G. Bertone, M. Cirelli, A. Strumia and M. Taoso, *JCAP* **0903**, 009 (2009) [arXiv:0811.3744 [astro-ph]].

- [19] S. Galli, F. Iocco, G. Bertone and A. Melchiorri, *Phys. Rev. D* **80**, 023505 (2009) [arXiv:0905.0003 [astro-ph.CO]]; T. R. Slatyer, N. Padmanabhan and D. P. Finkbeiner, arXiv:0906.1197 [astro-ph.CO].
- [20] R. Franceschini, T. Hambye and A. Strumia, *Phys. Rev. D* **78**, 033002 (2008) [arXiv:0805.1613 [hep-ph]].
- [21] F. del Aguila and J. A. Aguilar-Saavedra, *Nucl. Phys. B* **813**, 22 (2009) [arXiv:0808.2468 [hep-ph]].
- [22] A. Arhrib, B. Bajc, D. K. Ghosh, T. Han, G. Y. Huang, I. Puljak and G. Senjanovic, arXiv:0904.2390 [hep-ph].
- [23] T. Li and X. G. He, arXiv:0907.4193 [hep-ph].
- [24] C. H. Chen, M. Drees and J. F. Gunion, *Phys. Rev. Lett.* **76**, 2002 (1996) [arXiv:hep-ph/9512230]; J. L. Feng, T. Moroi, L. Randall, M. Strassler and S. f. Su, *Phys. Rev. Lett.* **83**, 1731 (1999) [arXiv:hep-ph/9904250].
- [25] P. Fileviez Perez, H. H. Patel, M. J. Ramsey-Musolf and K. Wang, *Phys. Rev. D* **79**, 055024 (2009) [arXiv:0811.3957 [hep-ph]].
- [26] S. Giagu, “Search for long lived particles in ATLAS and CMS”, Talk presented at ICHEP 2008, Philadelphia, PA; The ATLAS Collaboration, “Expected Performance of the ATLAS Experiment : Detector, Trigger and Physics”, CERN-OPEN-2008-020 [arXiv:0901.0512 [hep-ex]]; The CMS Collaboration, “Search for heavy stable charged particles with 100/pb and 1/fb in the CMS experiment”, CMS-PAS-EXO-08-003.